# Micromachined 100GHz near-field measurement probe for high-resolution microwave skin-cancer diagnosis

Fritzi Töpfer, Sergey Dudorov, Joachim Oberhammer

KTH Royal Institute of Technology, SE-100 44 Stockholm, Sweden; Email: fritzi@kth.se

***Abstract* — This paper reports for the first time on a novel micromachined millimeter-wave near-field measurement probe for skin-cancer diagnosis, which is designed for high lateral resolution for resolving small skin cancer speckles as well as for vertically discriminating shallow tissue-layer anomalies. A tip size as small as 0.18 mm$^2$, which is 18times smaller than conventional measurement tips for the design frequency of 100 GHz, could be achieved by micromachining a silicon-core tapered dielectric-rod waveguide. This metallized dielectric probe is positioned centrally into a standard WR-10 waveguide by a micromachined holder which allows for easily exchanging the probes at high reproducibility. The dielectric-wedge transition between the waveguide and the probe is optimized for 100-105 GHz. Furthermore, this paper presents a unique concept of micromachined test samples with tailor-made permittivity ranging from 1.7 to 7.1, which enables emulation of the different water content of tissue anomalies. This test method results in highly reproducible test measurements for evaluating and comparing different prototype probe designs. The paper presents successful measurement results of fabricated probes and test samples. Different single test samples as well as sample stacks with emulated tissue anomalies could clearly be distinguished.**

***Index Terms* — dielectric-rod waveguide, micromachining, microwave spectroscopy, near-field probe, skin cancer.**

## I. Introduction

Skin cancer, in particular malignant melanoma is the worldwide fastest growing cancer form, with incidence rates having been increasing by almost 3% per year since 2004 in the USA [1],[2]. More than 75,000 diagnoses of malignant melanoma are expected to be diagnosed in the USA for 2012, which will lead to more than 9000 deaths. Estimations for basal cell carcinoma (BBC) and squamous cell carcinoma (SCC) range from 1 Mio to 3.5 Mio new cases yearly in the USA [2]. As of today, there is no reliable skin cancer diagnosis sensor technology available, and diagnosis can only be carried out by experienced dermatologists.

Microwaves are able to discriminate cancer tissue, as energy absorption above 1 GHz is sensibly higher in cancerous than in healthy tissue which is attributed to the increased water content of tumors [3],[4], for instance from 60.9 to 81.7% [5]. Microwave/THz-wave probes are currently being tested for breast-cancer and intra-surgical cancer detection [6],[7]. However, microwave sensors for skin cancer diagnosis have so far failed, since skin cancer tumors are very shallow and inhomogeneous, so that conventional microwave probes approaches do not show enough spatial discrimination to the surrounding healthy tissue. Furthermore, a major problem in this sensor technology development is to have reproducible calibration samples for objective comparison of the measurement probe performance, as tissue samples are very inhomogeneous and very sensitive to parameters which are difficult to control, for instance humidity and contact pressure.

This paper reports for the first time on a novel, micromachined, high-resolution millimeter-wave near-field measurement probe of a tip size as small as 0.18 mm$^2$, including an optimized transition between a standard WR-10 waveguide and the micromachined dielectric-rod waveguide, optimized for 100-105 GHz. Furthermore, this paper presents a unique method of creating micromachined test samples of individual, tailor-made permittivity, which allows for emulating different skin layers with different properties, i.e. for mimicking thin cancer-tissue layers among healthy tissue. This test method results in highly reproducible test measurements for evaluating and comparing different probe tip designs.

## II. Need for Sub-millimeter Probe tips

The probability of metastasis and thus mortality increases drastically with increasing tumor size, especially if the thickness approaches 1 mm for malignant melanoma. Thus, tumors must be detected at an early stage, when their thickness is still not exceeding a few hundred micrometers. As illustrated in Figure 1, conventional coaxial probes and open rectangular waveguides in the W-band have a probe-tip size of the same magnitude as the wavelength, which is large as compared to inhomogeneous skin tumor speckles, and thus suffer from insufficient lateral solution. Furthermore, their size also results in a deep main interaction volume, which measures the average properties of the different vertical skin tissue layers and is not sufficiently able to discriminate shallow tumor layers. Moreover, it is important to match the

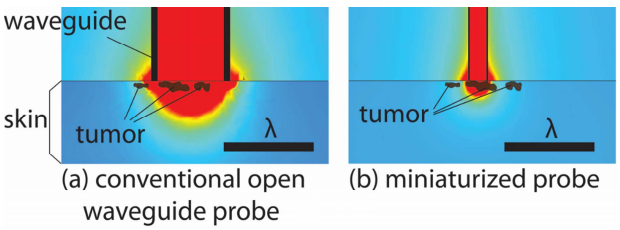


Fig. 1. Comparison of main interaction volume (red=half power density) of (a) conventional-sized rectangular waveguide probe, and (b) miniaturized high-permittivity core probe tip. Probe (b) has improved lateral resolution to discriminate tumor inhomogeneity and has higher sensitivity to the shallow cancer tissue layers (simulation with COMSOL Multiphysics).

probe to the permittivity values of tissue at the design frequency, to have high sensitivity for tissue anomalies.

Thus, there is a need for a substantially-miniaturized, sub-wavelength probe tip for diagnosing shallow skin tumors at an early stage and increasing survivability.

## III. Micromachined DRW Probe Design

The novel near-field probe concept, as shown in Figure 2, consists of a high-permittivity micromachined, metallized dielectric-rod waveguide (DRW) with a total length of 15.25 mm and a cross section of 0.6x1 mm$^2$. At the measurement tip, the DRW is tapered. This results in a drastically reduced probe tip size as small as 0.3x0.6 mm$^2$, which is only 5.6% of the cross-section of the feeding WR-10 waveguide (2.54x1.27 mm$^2$). The probe is fed via a tapered ending of the DRW inside the WR-10 waveguide. For a good transition of the electromagnetic wave, an exact positioning of the probe in the center, both horizontally and vertically, is critical. Therefore, a micromachined holder was fabricated in high resistivity silicon which allows for a precise and reproducible fitting of the probe inside the metal waveguide with a positioning accuracy much better than the fabrication tolerances of the metal waveguide itself. Additionally, the holder is designed in a way so that the probe can be exchanged, i.e. different probe tip designs can be evaluated.

The core of the DRW is high-resistivity silicon (>4000 Ωcm, $\varepsilon_r$=11.6, tan δ of $6 \times 10^{-4}$ measured at 100 GHz) and the RF design of the probe tip is done for matching the tip to the expected permittivity parameters of skin between 100 and 105 GHz ($\varepsilon_r$'=5.5 and $\varepsilon_r$"=5.4 for healthy, and $\varepsilon_r$'=6.5 and $\varepsilon_r$"=6.4 for cancerous skin tissue, for $\varepsilon_r = \varepsilon_r' - i\,\varepsilon_r''$, parameters from a 2nd order Debye skin-tissue model [8]). The matching is optimized for a nominal return loss of -10 dB for these parameters, as a compromise between good coupling into the test sample (low reflections) and high sensitivity to changes in the sample permittivity.

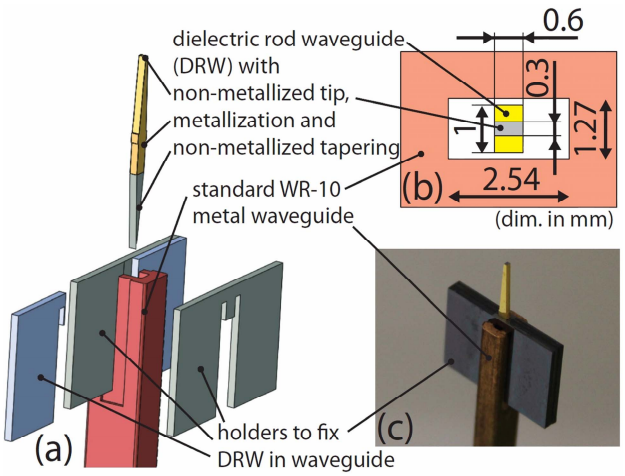


Fig. 2. Design of the DRW probe and its fixture in a standard metal waveguide: (a) exploded CAD drawing (b) schematic top view (c) photograph of device used for measurements.

The probes and the waveguide holders are fabricated in 600 µm thick high-resistivity silicon substrate, by deep-reactive ion etching using an inductively-coupled plasma etcher with a silicon dioxide hardmask. The DRW is metallized uniformly with 1.4 µm gold using a micromachined shadow mask in an electron-beam evaporator.

## VI. Test Sample Design and Micro-fabrication

In order obtain reproducible measurement results and to objectively test and compare different probe tip designs, skin-tissue layers are mimicked by micromachined, 300 µm thick silicon layers, as illustrated in Figure 3. The effective macroscopic permittivity of these silicon layers can be tailor-made by varying the size of etch holes in a periodic pattern which is substantially smaller than the wavelength.

TABLE I. Pitch, opening size and resulting permittivity for the fabricated test samples.

| *grid pitch p in µm* | *hole size h in µm* | *effective permittivity $\varepsilon_{eff}$* |
|---|---|---|
| 100 | 47 | 7.1 |
| 100 | 51 | 6.6 |
| 100 | 66 | 4.9 |
| 100 | 70 | 4.5 |
| 100 | 72 | 4.2 |
| 100 | 80 | 3.3 |
| 100 | 87 | 2.5 |
| 100 | 88 | 2.4 |
| 100 | 92 | 1.9 |

$$\epsilon_{eff} = \left(\frac{p-h}{h}\frac{1}{\epsilon_{Si}} + 1\right)^{-1} + \epsilon_{Si}\frac{p-h}{p}$$

The test samples were fabricated both in high resistivity silicon (>4000 Ωcm) and in silicon wafers of a measured resistivity of 480 Ωcm. The resulting effective permittivity, depending on the etch hole size, is listed in Table I. The values resemble the permittivity of skin tissue with different water content. The samples were stacked for the measurements to up to 4 layers (1.2 mm total thickness), for mimicking tumor layers within healthy skin tissue layers of different thicknesses and at varying depth. These test samples have, in contrast to polymer phantom materials or tissue samples, which have a

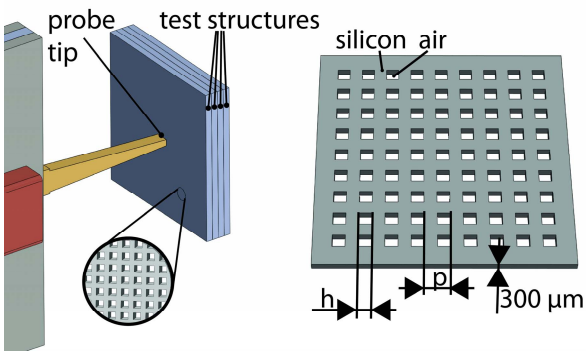


Fig. 3. Schematic drawing of a test sample with tailor-made permittivity (right) and of the measurement setup on a stack consisting of four test samples (left).

strong dependency on humidity, pressure and other parameters, a reproducibility of the measurement results in the order of 3.5%.

## V. Measurement Results

Reflection measurements were conducted using an Agilent E8163A vector network analyzer (VNA) with millimeter-wave measurement heads up to 110 GHz. The rectangular waveguide with the inserted DRW was connected to the VNA and the return loss $S_{11}$ was measured while the probe tip was put in contact with the test samples.

Figure 4 shows the return loss ($S_{11}$) measurements on single-layer test samples of different effective permittivity. These measurements were carried out on fabricated samples of substrate resistivity of 480 Ωcm and of >4000 Ωcm. As expected, a clear dependency of the reflections on the permittivity can be seen.

In Figure 5 the results of measurements with a probe of a tip size of 0.4x0.6 mm$^2$ on stacks of test sample layers can be seen. The reflections are lower for the stacks where the first or the first and the second layer have a higher permittivity, mimicking the significantly higher water content of a tumor in these layers, compared to the stack with uniform permittivity, mimicking healthy skin. For the measurement where only the second layer has a higher permittivity $S_{11}$ differs only slightly from the uniform stack. That suggests that mainly the superficial layer(s) have an influence on the measurement and the measurement will not be influenced by deeper skin layers. This can be advantageous for detecting thin tumors close to the surface.

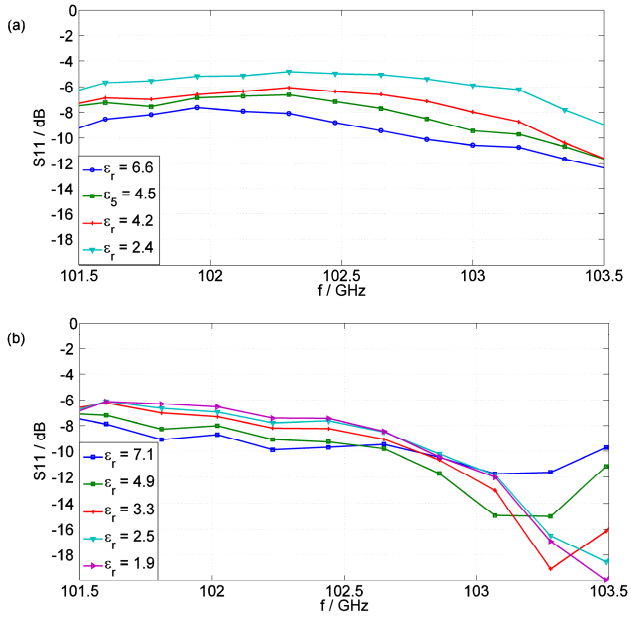


Fig. 4. Measurements of single-layer test samples of different permittivity $\varepsilon_r$: (a) test samples consisting of >4000 Ωcm silicon; and (b) 480 Ωcm silicon.

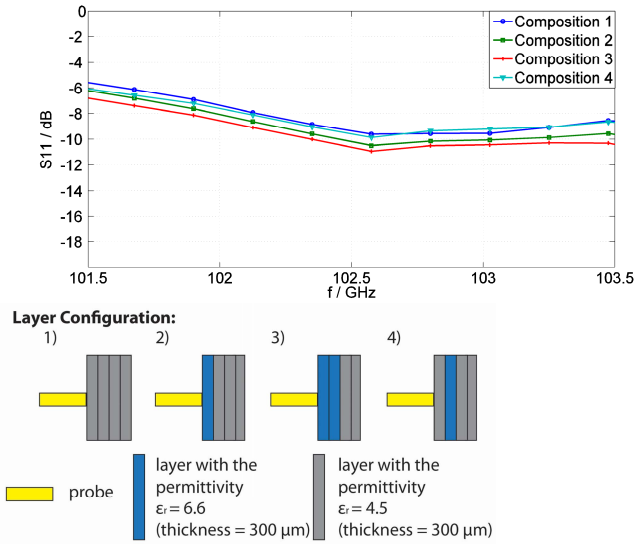


Fig. 5. Measurement of different stacks of test samples using a probe with tip size of 0.6x0.4 mm$^2$, for investigating the sensitivity of the probe to shallow-layer tissue anomalies.

## VI. Conclusion

This paper presented a new, micromachined, high-resolution microwave measurement probe for skin-cancer diagnosis, and on a novel method of creating test samples with tailor-made permittivity, for mimicking tissue layers of different microwave properties. The probes were able to successfully distinguish different artificial test samples and could discriminate mimicked tissue anomalies in multi-layer samples.

## References


[1] K. Nouri, *Skin cancer*, New York: McGraw-Hill Medical, 2008.

[2] American Cancer Society. *Cancer Facts & Figures 2012*. Atlanta: American Cancer Society, 2012.

[3] J.L. Schepps and K.R. Foster, "The UHF and microwave dielectric properties of normal and tumour tissues: variation in dielectric properties with tissue water content," *Physics in Medicine and Biology*, vol. 25, 1980, pp. 1149-1159.

[4] V.P. Wallace, A.J. Fitzgerald, E. Pickwell, R.J. Pye, P.F. Taday, N. Flanagan, and T. Ha, "Terahertz Pulsed Spectroscopy of Human Basal Cell Carcinoma," *Applied Spectroscopy*, vol. 60, 2006, pp. 1127-1133.

[5] V. Stuntzeff, C. Carruthers, "The water content in the epidermis of mice undergoing carcinogenesis by methylcholanthrene", *Cancer Res*., vol. 6, pp. 574/577, 1946.

[6] www.dunemedical.com

[7] http://www.teraview.com/applications/medical/oncology.html

[8] E. Pickwell, A.J. Fitzgerald, B.E. Cole, P.F. Taday, R.J. Pye, T. Ha, M. Pepper, and V.P. Wallace, "Simulating the response of terahertz radiation to basal cell carcinoma using ex vivo spectroscopy measurements," *Journal of Biomedical Optics*, vol. 10, 2005, p. 064021.